Article:
Haque, N orcid.org/0000-0002-0271-9209, Cochrane, RF and Mullis, AM (2018) Order-disorder morphologies in rapidly solidified ε/ε′-Ni_5Ge_3 intermetallic. Journal of Alloys and Compounds, 739. pp. 160-163. ISSN 0925-8388

https://doi.org/10.1016/j.jallcom.2017.12.253

Order-disorder morphologies in rapidly solidified ε/ε'-Ni_5Ge_3 intermetallic

Nafisul Haque[1, a], Robert F. Cochrane[1], Andrew M. Mullis[1]
[1] School of Chemical & Process Engineering, University of Leeds, Leeds LS2 9JT, UK
[a]Corresponding author: pmnh@leeds.ac.uk, R.F.Cochrane@leeds.ac.uk, A.M.Mullis@leeds.ac.uk
Keywords: rapid solidification; intermetallic compound; plate & lath microstructure

Abstract

Congruently melting, single-phase Ni_5Ge_3 (T_m = 1185 °C) has been rapidly solidified via drop-tube processing wherein powders, with diameters between 850 – 53 μm, are produced. At low cooling rates (850 – 150 μm diameter particles, 700 – 7800 K s^{-1}) the dominant solidification morphology, revealed after etching, is that of isolated plate & lath microstructure in an otherwise featureless matrix. At higher cooling rates (150 – 53 μm diameter particles, 7800 – 42000 K s^{-1}) the dominant solidification morphology is that of isolated faceted hexagonal crystallites, again imbedded within a featureless matrix. Selected area diffraction analysis in the TEM reveals the plate & lath, and isolated hexagonal crystallites, are a disordered variant of ε-Ni_5Ge_3, whilst the featureless matrix is the ordered variant of the same compound. Thermal analysis and *in situ* heating in the TEM indicate a reversible solid-state order-disorder transformation between 470 - 485 °C.

1. Introduction

Intermetallic compounds have been of widespread and enduring interest within Materials Science over the last 30 years or so. Such compounds are characterised by strong internal order and mixed covalent/ionic and metallic bonding, which gives rise to mechanical behaviour intermediate between ceramics and metals. A range of potential applications as high temperature structural materials have been proposed for these materials due to good chemical stability and high hardness at elevated temperatures. However, poor room temperature ductility limits formability. Such limitations can be overcome by controlling the degree of chemical ordering present within the intermetallic, with the disordered form typically showing behaviour which is more metallic in character (higher ductility, lower hardness, and lower chemical resistance) than the fully ordered form. Rapid solidification of intermetallics is therefore an important area of study as high cooling rates are one means of suppressing ordering. Subsequent annealing of the formed part can then be utilised to restore chemical ordering, and hence the desirable properties of the intermetallic.

In this paper we consider the rapid solidification of the intermetallic Ni_5Ge_3. This is an interesting model system as, being congruently melting, the ordering reaction can be studied without any complicating solute effects. That is, we can be certain that solute partitioning, and hence also solute trapping, is absent.

The phase diagram for the Ni-Ge system has been studied extensively by Ellner et al. [1] and by Nash and Nash [2], in 1971 and 1987 respectively. More recently, further work has been also reported by Liu *et al.* [3] and by Jin *et al.* [4]. Ni_5Ge_3 is a congruently melting compound with a homogeneity range for the single phase compound of 34.6 – 44.5 at.% Ge. The congruent point is towards the Ge-deficient end of this range at 37.2 at.% Ge and 1458 K. Ni_5Ge_3 displays two equilibrium crystalline forms, ε and ε' [2] [4]. The high temperature ε-phase has the $P6_3/mmc$ crystal structure (Hexagonal, space group 194), while the low temperature ε'-phase has the C2 crystal structure (Monoclinic, space group 5) [4]. The transition between the two occurs either

congruently ($\varepsilon \rightarrow \varepsilon'$) at 670 K for Ge-rich compositions or via the eutectoid reaction $\varepsilon \rightarrow \varepsilon' + \delta$ at 560 K for Ge-deficient compositions. No order-disorder transitions are shown on the phase diagram and as far as we are aware it is not known whether the high temperature ε phase orders direct from the liquid upon solidification or in the solid-state at some temperature below the liquidus.

In this article we present an analysis of rapidly solidified Ni-37.2 at%. Ge, which is close to the notional stoichiometry of the Ni_5Ge_3 compound. Rapid solidification was affected via drop-tube processing, in which cooling rate is primarily determined by particle size. The main objective of the study is to determine whether ordering occurs upon solidification, or in the solid-state at some temperature below the liquidus and to elucidate the effect of cooling rate on suppressing the ordering reaction. Two very different microstructures were observed; plate & lath type structure were observed at low cooling rates (700 – 7800 K s^{-1}, 850 – 150 μm diameter particles) while at higher cooling rates (7800 – 42000 K s^{-1}, 150 – 53 μm diameter particles) isolated faceted hexagonal crystallites in an otherwise featureless matrix were observed.

2. Experimental Methods

Elemental Ni and Ge were obtained from Alfa Aesar with purity of 99.99 % and 99.999% (metals basis) respectively. Single phase Ni_5Ge_3, of composition Ni-37.2 at. % Ge, was produced by arc-melting the elemental constituents together under a protective argon atmosphere. The phase composition of the subsequent ingot was confirmed by XRD using a PANalytical Xpert Pro. The data were collected over a range of 20-100° in 2θ using Cu-K_α radiation (λ = 0.15418 nm) generated at an anode voltage of 40 kV and with a current of 40 mA. Only after confirmation that the ingot was single phase Ni_5Ge_3 was rapid solidification processing undertaken.
Rapid solidification was affected by drop-tube processing, using a 6.5 m drop-tube. The tube was rough pumped to a pressure of 2 x 10^{-4} Pa before being flushed with N_2 gas. The rough pump – flush cycle was repeated three times before the tube was evacuated to a pressure of 4 x 10^{-7} Pa using a turbo-molecular pump. For sample processing the tube was filled with dried, oxygen free N_2 gas at a pressure of 50 kPa. The alloy sample, of approximately 9.4 g mass was loaded into an alumina crucible which has three 300 μm laser drilled holes in the base. Induction heating of a graphite subsector was used for heating the sample. Temperature determination was by means of an R-type thermocouple which sits inside the melt crucible, just above the level of the melt. When the temperature in the crucible attained 1533 K (75 K superheat) the melt was ejected by pressuring the crucible with ~ 400 kPa of N_2 gas. This produces a fine spray of droplets which subsequently solidify in-flight and are collected at the base of the tube.

The sample was weighed following removal from the drop-tube and sieved into the following size fractions: ≥ 850 μm (< 700 K s^{-1}), 850 - 500 μm (700 - 1400 K s^{-1}), 500 - 300 μm (1400 - 2800 K s^{-1}), 300 - 212 μm (2800 - 4600 K s^{-1}), 212 - 150 μm (4600 - 7800 K s^{-1}), 150 - 106 μm (7800 - 13000 K s^{-1}), 106 - 75 μm (13000 - 26000 K s^{-1}), 75 - 53 μm (26000 - 42000 K s^{-1}), 53 - 38 μm (42000 - 62000 K s^{-1}) and ≤ 38 μm (> 62000 K s^{-1}). For each size fraction the cooling rate, calculated using the methodology described in [5], is shown in brackets.

All of drop-tube powders were subject to XRD analysis to ensure they remained single-phase prior to further analysis. Each sieve fraction was then mounted in transoptic resin and prepared for microstructural analysis using OM (Olympus BX51) and SEM (Carl Zeiss EVO MA15 scanning electron microscope). For such analysis samples were etched for 25 seconds in a mixture of equal parts of undiluted HNO_3 + HCl + HF. An Oxford Instrument X-Max Energy-Dispersive X-Ray (EDX) detector was used to check the chemical homogeneity of the etched samples.

In addition to microstructural analysis using OM and SEM, bright-field imaging and selected area diffraction analysis in the transmission electron microscopy (TEM), using an FEI Tecnai TF20, was used to distinguish between the ordered and disordered variants of the ε and ε' phases. For in situ observation of the order-disorder transformation upon heating the TEM was fitted with a Gatan 901 hot stage controller. Samples were prepared for TEM analysis using an FEI Nova 200 Nanolab focused ion beam (FIB), with the sections cut being approximately 10 μm × 7 μm and between 55-70 nm in thickness. An example of a FIB milled section for the related β-Ni_3Ge compound is shown in [6]. Thermal analysis using a Perkin Elmer STA 8000 was undertaken to identify the transition temperature for the ordered to disorder reaction, with a temperature scanning range from room temperature to 1085 °C with a heating/cooling rate of 10 K min^{-1}.

3. Results & Discussion

XRD data for three of the sieve fractions is shown in Figure 1, together with the ICCD reference patterns for ε-Ni_5Ge_3 (04-004-7264) and ε'- Ni_5Ge_3 (01-075-6729). From the XRD patterns it is clear that all samples are Ni_5Ge_3. Many of the peaks for the ε- and ε'-phases occupy similar positions, although the strong double peaks that occur in the spectrum of the ε-phase at 44.72° and 46.28° are shifted to slightly higher angles (45.48° and 46.65°) for the ε'-phase, allowing an unambiguous identification. The ≥ 850 μm sieve fraction we identify as the equilibrium (low temperature) ε'-phase and the 850-500 μm sieve fraction, together with all smaller size fractions, being the high temperature ε-phase. It would seem likely therefore that cooling rates in excess of 700 K s^{-1} are sufficient to suppress the ε → ε' transition, resulting in the retention of the metastable ε-phase down to room temperature.

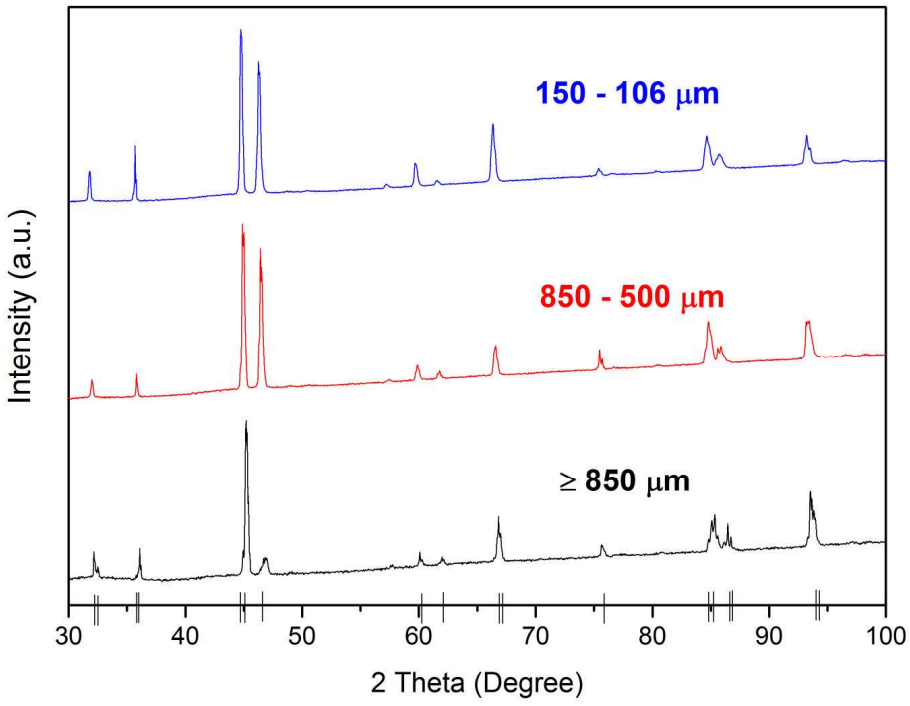

Figure 1: X-Ray diffraction analysis of rapidly solidified drop-tube processed samples, ≥ 850 μm size (black), 850 -500 μm size range (red) and 150 -106 μm size range (blue) respectively. Vertical black lines indicate peak positions for the ε- Ni_5Ge_3 /ε'- Ni_5Ge_3 reference pattern.

Figure 2(a) shows an SEM micrograph of a polished and HF etched sample in a powder from the 500 - 300 µm sieve fraction, wherein numerous plate & lath like structures are evident. Such structures remain the dominant morphology until the particle size drops below 150 µm wherein the plate & lath structure is replaced by numerous isolated faceted hexagonal crystallites in a more-or-less uniform featureless matrix. An example of this is shown in Figure 2(b) for the 150 -106 µm sieve fraction. Plate & lath structures are relatively common in intermetallic compounds [7-9] and also in some iron alloys [10]. Hyman *et al*. observed plate & lath structures in γ-TiAl [7] resulting from the solid-state transformation of α dendrites during cooling to a mixture of α_2 + γ laths surrounded by γ segregates. McCullough *et al.* also reported plate and lath morphology in α_2-Ti_3Al which, like ε-Ni_5Ge_3, shares the $P6_3/mmc$ space group [8].

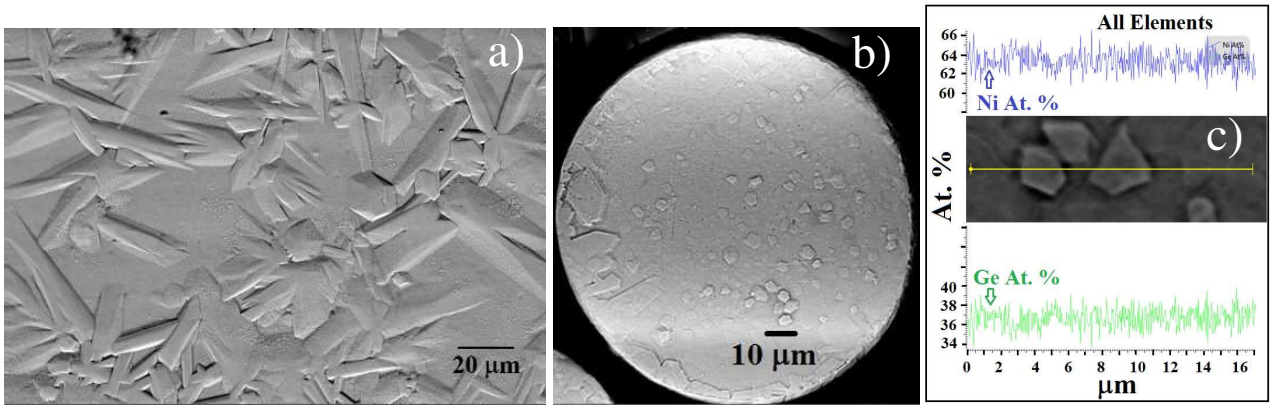

Figure 2 : (a) SEM micrograph of HF etched Ni_5Ge_3 drop-tube particle from (a) the 500 – 300 µm size fraction showing numerous plate and lath structures and (b) from the 150 – 106 µm size fraction showing isolated faceted crystallites in a more-or-less featureless matrix (c) EDX line scan across the diameter of droplet from the 150 – 106 µm size fraction, showing that the contrast revealed by etching is not the result of solute partitioning.

However, in other materials that display the plate and lath structure, such as Ti_3Al, it is clear that this morphology arises due to contrast between different phases. This cannot be the case here as the material is single phase. Nor, for a congruently melting compound, would we expect the contrast to be due to differences in composition of the solid. The absence of solute partitioning is demonstrated in Figure 2(c), which shows an EDX line scan across some of the isolated hexagonal crystallites. From this it is clear that, to within the experimental error associated with the technique, there is little variation in composition between the structures revealed by etching and the surrounding featureless matrix. The same is true in the plate and lath morphology, EDX shows these to be chemically homogeneous. The contrast revealed by etching does not therefore appear to be related to differences in either phase (XRD) or chemical composition (EDX).

In order to understand the origin of morphologies revealed by etching in the rapidly solidified Ni_5Ge_3 drop-tube samples TEM imaging and Selected Area Diffraction (SAD) analysis has been performed. Figure 3a shows a TEM bright field image of a FIB section through a lath & plate structure and some of the immediately surrounding matrix material. Two regions are identified in part (a) for SAD analysis; (i) matrix materials away from the plate & lath structure and (ii) inside the plate & lath structure. The results of SAD analysis from regions (i) and (ii) are shown in Figure 3 b-c respectively. In Figure 3b supper-lattice spots are clearly evident, indicating the matrix material to be chemically ordered, whereas in Figure 3c the supper-lattice spots are absent, indicating the material comprising the plate and lath morphology to be chemically disordered. Similar results were obtained on a FIB section cut from a particle in the 150 – 106 µm size fraction, displaying the isolated faceted crystallite structure, although for the sake of brevity that is not

reproduced here. Consequently, we conclude that the contrast revealed by etching is due to incomplete chemical ordering, with the etchant preferentially attacking the disordered material while leaving the ordered material intact. Similar behaviour has been observed in other Ni-Ge alloys [11, 12].

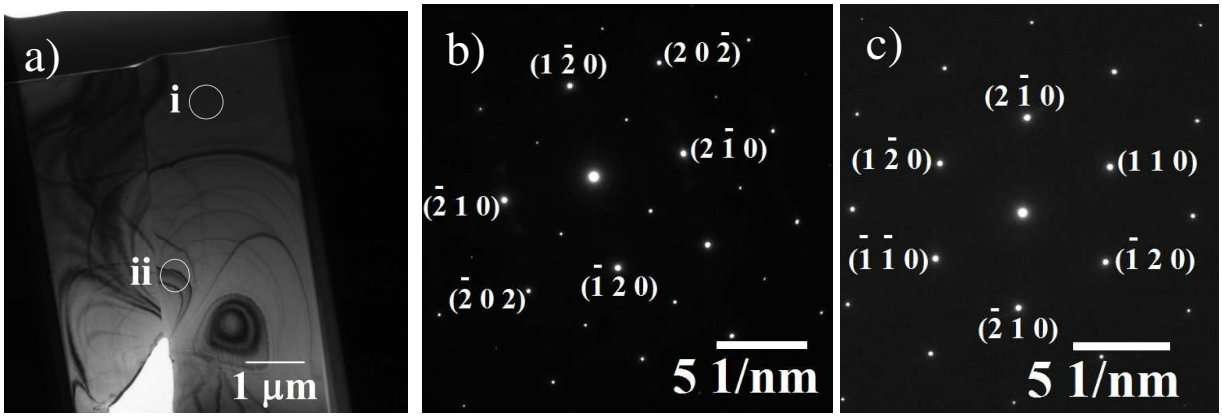

Figure 3: (a) TEM bright field image of a plate & lath structure and surrounding matrix material in a 500 – 300 µm size fraction, (b and c) selected area diffraction patterns from regions (i) with zone axis [2, 1, 2] and (ii) with zone axis [0, 0, 1] identified in the bright field image (i) matrix materials well away from the plate & lath structure, (ii) inside the structure.

In order to determine whether ordering occurs in the solid-state or upon solidification at the liquidus temperature differential scanning calorimetry (DSC) was performed on powders from the 150 – 106 µm size fraction, the results of which are given in Figure 4a. Two low temperature transformations are apparent. The first of these appears to be 300 – 320 °C and from the phase diagram is likely to be the $\varepsilon \rightarrow \varepsilon' + \delta$ eutectoid, as would be expected for material at 37.2 at% Ge. In this respect it is interesting to note that the largest drop-tube sieve fraction, powders > 850 µm, was single phase ε'. This suggests that cooling was sufficiently rapid to suppress the $\varepsilon \rightarrow \varepsilon' + \delta$ eutectoid, forcing the system to undergo the congruent $\varepsilon \rightarrow \varepsilon'$ transition instead. The second low temperature transition visible in the DSC appears to be 460 – 540 °C, which we postulate may be associated with the order-disorder transformation in the high temperature ε-phase. To confirm this an *in situ* heating experiment has been performed in the TEM. An initially ordered region, corresponding to the featureless matrix material, was selected and the SAD pattern obtained in order to ensure the material was indeed ordered (Figure 4b). The material was then progressively heated until the super-lattice spots vanished, indicating the material had transformed to the fully disordered phase, wherein the temperature was 485 °C, consistent with the peak in the DSC curve.

It would therefore appear that during the solidification of an Ni-37.5 at. % Ge melt the primary solidification phase is the disordered variant of the high temperature ε-Ni_5Ge_3 phase. Upon cooling this would be expected to undergo a disorder-order transformation in the solid-state around 485 °C, but that cooling rates in excess of 700 K s^{-1} can partially suppress ordering, resulting in the partially ordered structures shown in Figure 2a-b. At these cooling rates the transformation to ε' is also suppressed, resulting in retained, metastable ε at room temperature. For cooling rates below 700 K s^{-1} it appears that the transformation to the low temperature ε'-phase is not suppressed, although this may be forced to occur via the congruent $\varepsilon \rightarrow \varepsilon'$ transition, rather than via the $\varepsilon \rightarrow \varepsilon' + \delta$ eutectoid reaction.

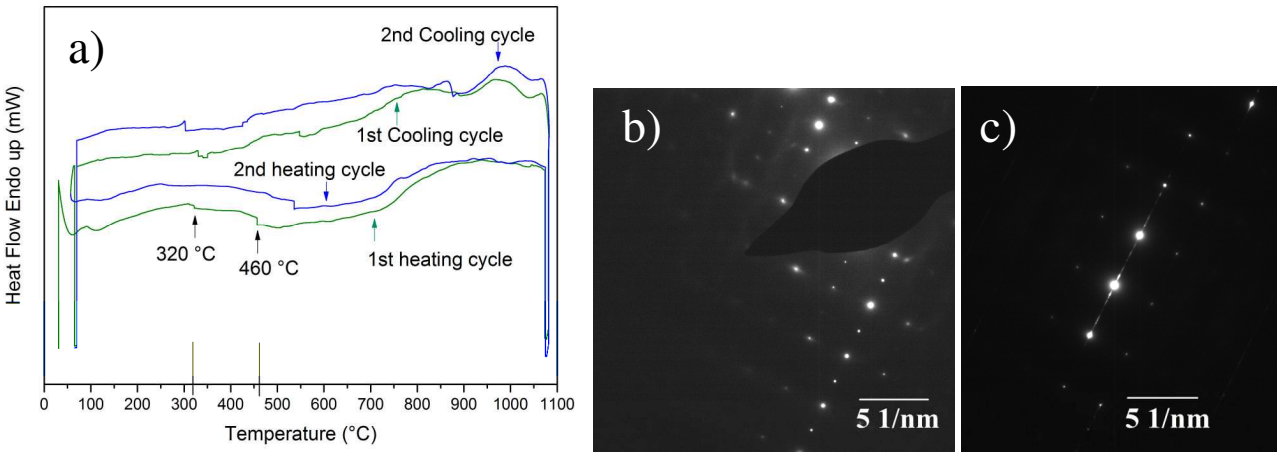

Figure 4: (a) DSC trace from a Ni_5Ge_3 drop-tube particle from the 150 – 106 µm size fraction, 1st & 2nd cycle indicated by green & blue respectively, two vertical black line shows the transition temperature at 320 to 460 °C and (b) TEM (*In-situ)* SAD pattern taken from Figure 2(b) at room temperature (ordered) and (c) SAD of the same area but at 485 °C (disordered).

4. Summary & Conclusion

Congruently melting, single-phase Ni_5Ge_3 has been rapidly solidified via drop-tube processing. All drop-tube samples were confirmed to have remained single-phase Ni_5Ge_3. In all powder sizes except the largest sieve fraction (> 850 µm) the high temperature ε-phase was found to be retained upon cooling to room temperature. Within the ε-phase it was found that at low cooling rates (850 – 150 µm diameter particles, 700 – 7800 K s^{-1}) the dominant solidification morphology, revealed after etching, is that of isolated plate & laths within a featureless matrix. At higher cooling rates (150 – 53 µm diameter particles, 7800 – 42000 K s^{-1}) the dominant solidification morphology is that of isolated hexagonal crystallites also within a featureless matrix. Selected area diffraction analysis in the TEM reveals the plate & laths and isolated hexagonal crystallites are a disordered variant of ε-Ni_5Ge_3, whilst the featureless matrix is the ordered variant of the same compound. Differential scanning calorimetry (DSC) indicates two low temperatures transformations. The first of these appears between 300 – 320 °C and is likely to be the $\varepsilon \rightarrow \varepsilon' + \delta$ eutectoid decomposition. The second appears to be in the range 460 – 540 °C and we postulate may be associated with the order-disorder transformation in the high temperature ε-phase. An *in situ* heating in the TEM also indicated a solid-state order-disorder transformation between 470 - 485 °C, with the material transforming to the fully disordered phase above 485 °C.

Acknowledgments

Nafisul Haque is thankful to the Higher Education Commission (HEC) Pakistan and NED University of Engineering & Technology for financial support.

References

[1] M. Ellner, T. Gödecke, K. Schubert, Zur struktur der mischung Nickel-Germanium, Journal of the Less Common Metals, 24 (1971) 23-40.

[2] A. Nash, P. Nash, The Ge− Ni (Germanium-Nickel) system, Journal of Phase Equilibria, 8 (1987) 255-264.

[3] Y. Liu, D. Ma, Y. Du, Thermodynamic modeling of the germanium–nickel system, Journal of Alloys and Compounds, 491 (2010) 63-71.
[4] S. Jin, C. Leinenbach, J. Wang, L.I. Duarte, S. Delsante, G. Borzone, A. Scott, A. Watson, Thermodynamic study and re-assessment of the Ge-Ni system, Calphad, 38 (2012) 23-34.
[5] O. Oloyede, T.D. Bigg, R.F. Cochrane, A.M. Mullis, Microstructure evolution and mechanical properties of drop-tube processed, rapidly solidified grey cast iron, Materials Science and Engineering: A, 654 (2016) 143-150.
[6] N. Haque, R.F. Cochrane, A.M. Mullis, Rapid solidification morphologies in Ni_3Ge: Spherulites, dendrites and dense-branched fractal structures, Intermetallics, 76 (2016) 70-77.
[7] M. Hyman, C. McCullough, J. Valencia, C. Levi, R. Mehrabian, Microstructure evolution in TiAl alloys with B additions: conventional solidification, Metallurgical Transactions A, 20 (1989) 1847.
[8] C. McCullough, J. Valencia, C. Levi, R. Mehrabian, Microstructural analysis of rapidly solidified Ti □ Al X powders, Materials Science and Engineering: A, 124 (1990) 83-101.
[9] T. Broderick, A. Jackson, H. Jones, F. Froes, The effect of cooling conditions on the microstructure of rapidly solidified Ti-6Al-4V, Metallurgical Transactions A, 16 (1985) 1951-1959.
[10] G. Krauss, A. Marder, The morphology of martensite in iron alloys, Metallurgical and Materials Transactions B, 2 (1971) 2343-2357.
[11] N. Haque, R.F. Cochrane, A.M. Mullis, Disorder-order morphologies in drop-tube processed Ni_3Ge: Dendritic and seaweed growth, Journal of Alloys and Compounds, (2016).
[12] N. Haque, R.F. Cochrane, A.M. Mullis, Morphology of Order-Disorder Structures in Rapidly Solidified L12 Intermetallics, in: TMS 2017 146th Annual Meeting & Exhibition Supplemental Proceedings, Springer, 2017, pp. 729-736.